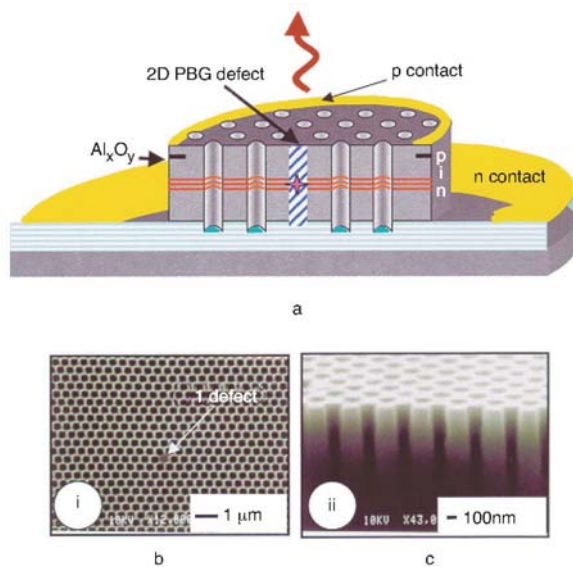


# Electrically injected single-defect photonic bandgap surface-emitting laser at room temperature

W.D. Zhou, J. Sabarinathan, B. Kochman, E. Berg, O. Qasaimeh, S. Pang and P. Bhattacharya

An electrically injected defect-mode photonic bandgap microcavity surface-emitting laser at room temperature is demonstrated for the first time. 931 nm lasing is observed under pulsed excitation conditions, with a threshold current of 300  $\mu$ A. Near- and far-field modal characteristics of the emission confirm lasing from the defect-related microcavity in the photonic bandgap crystal.

Light sources that display reasonably high power efficiency, together with singlemode operation, narrow spectral linewidth, and directional output will be extremely useful for array applications where high fibre coupling efficiency and low crosstalk are essential [1]. A vertical-cavity surface-emitting laser (VCSEL) is an example of a  $\lambda$ -sized cavity and, with additional lateral confinement by wet-oxidation of  $\text{Al}_x\text{Ga}_{1-x}\text{As}$  layers, three-dimensional mode confinement can be obtained. The micro-disk laser is another example. However, the most appealing technique to realise a true photonic microcavity is to use a dielectric photonic crystal, with a 'lattice' defect in the photonic bandgap (PBG), which traps the photon modes [2 – 4]. Optically pumped PBG defect mode surface-emitting lasers have been demonstrated recently [5, 6]. We report here 0.9  $\mu\text{m}$  lasing in a  $p$ - $n$  junction 2D-PBG defect mode surface-emitting laser with electrical injection by incorporating a bottom DBR mirror and deep dry etching technique.



**Fig. 1** Schematic diagram of laser and SEM images of photonic crystal

- a Schematic diagram of electrically injected photonic crystal microcavity laser
- b Scanning electron micrograph images of top view and cross-sectional view of photonic crystal through the active region with single defect
  - (i) top view
  - (ii) cross-sectional view

The device heterostructure was grown by metal-organic vapour phase epitaxy (MOVPE). It consists of an  $n^+$  GaAs contact layer, an  $n$ -type lower 29 pair GaAs/ $\text{Al}_{0.80}\text{Ga}_{0.20}\text{As}$  distributed Bragg reflector (DBR) mirror, an undoped  $\lambda$  cavity region with two 70  $\text{\AA}$  pseudomorphic  $\text{In}_{0.15}\text{Ga}_{0.85}\text{As}$  wells in the middle and  $p$ -type AlGaAs and contact layers on the top.  $n$ - and  $p$ -type  $\text{Al}_{0.96}\text{Ga}_{0.04}\text{As}$  layers are also inserted on the respective sides of the cavity region for eventual lateral wet-oxidation during device processing. The bottom DBR is not essential, but is incorporated to achieve a high index step and ensure leakage of light from the top surface. The reflectivity of the top surface, on the other hand, is simply provided by the semiconductor-air interface. The luminescence measured from the InGaAs quantum well exhibits a peak emission at 940 nm at room temperature.

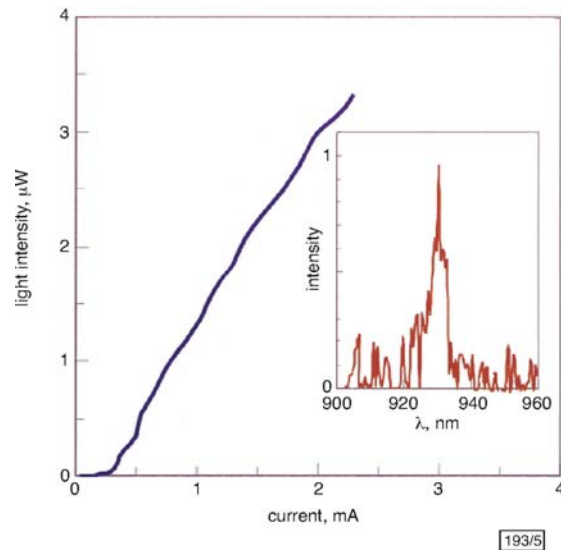


**Fig. 2** Light-current characteristics of pulsed single-defect PBG laser at 300 K

Inset: Spectral output at  $I = 5 \text{ mA}$

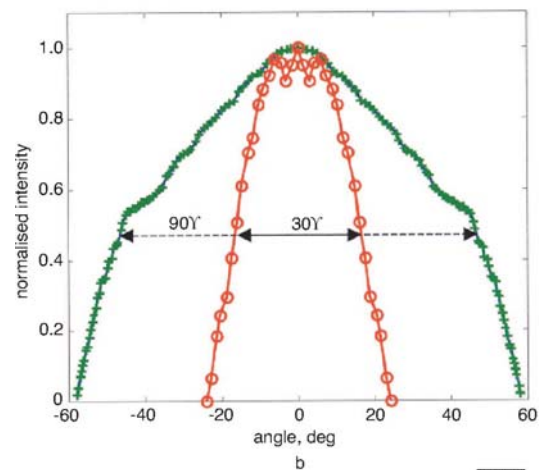
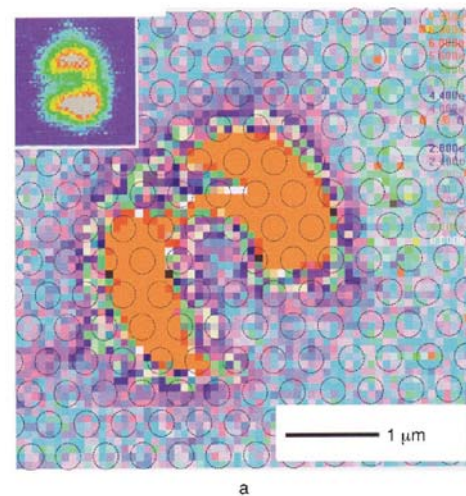


**Fig. 3** Near-field image of laser output and far-field pattern with and without photonic crystals

- a Measured near-field image of laser output, with 2D air-hole photonic crystal pattern shown
- b Far-field pattern for devices without and with photonic crystals
  - device with photonic crystal
  - + device without photonic crystal

Device fabrication begins with the design of the PBG crystal with a defect in the centre. The cavity was designed with a PBG encompassing the peak emission wavelength at a normalised frequency of  $a/\lambda$  for the TE modes. In our case, the PBG centre frequency is  $a/\lambda = 0.426$ , which corresponds to the peak wavelength of  $0.94\mu\text{m}$ . Standard oxide-confined VCSEL process steps were used in the device fabrication with a combination of optical lithography, dry and wet etching, metallisation and polyimide planarisation. The  $\text{Al}_x\text{O}_y$  regions created by wet oxidation help to funnel the charge carriers more efficiently into the centre of the PBG region. The 2D PBG formation is subsequently achieved by e-beam lithography, pattern transfer and deep dry etching techniques [7]. The deep etch ( $\sim 0.8\mu\text{m}$  deep) goes through the entire cavity region, and well into the bottom DBR to ensure a good overlap with the optical field. Single or multiple defects in the centre define the  $\lambda$ -sized microcavity. As shown in Fig. 1b, the lattice constant of the 2D PBG is  $a = 0.4\mu\text{m}$ , with the ratio of the air hole radius to the lattice constant,  $r/a = 0.32$ . The active area aperture, created by the single defect, is surrounded by over 40 periods of PBG, having an extent (radius) of  $20\mu\text{m}$ .

The devices were tested in the pulsed mode via probe contacts, without any heat sinking. The output light-current (L-I) and spectral characteristics are shown in Fig. 2. The output was measured in a direction normal to the surface. It should be remembered that the dominant mode in the defect region can propagate laterally, or leak out vertically. The DBR mirror at the bottom assists surface emission from the top. The threshold current is  $300\mu\text{A}$  and the maximum measured output power is  $14.4\mu\text{W}$ . The peak emission in the spectral output at  $931\text{nm}$  has a linewidth of  $8\text{\AA}$ , resulting in a Q of  $\sim 1164$ . It is known that the output from a microcavity formed by removing a single air-hole in a PBG crystal is a pair of degenerate modes [8]. These may be present in the output spectrum. The peak output wavelength corresponds to a normalised frequency of  $0.43$ , which is within the bandgap of the photonic crystal incorporated in our device. While the PL peaks at  $940\text{nm}$  at  $300\text{K}$ , the output emission centre wavelength is  $931\text{nm}$ . The shift is mainly due to the process induced PBG position and defect level shift.

It is necessary to ensure that the measured output at  $931\text{nm}$  results from microcavity effects in the single defect and that the entire 2D-PBG crystal beyond the defect microcavity does not contribute to the lasing. The following features lead us to believe that the device operates as a defect mode laser. Photoluminescence measurements were carried out and the peak intensity of PL spectra from the PBG region was 10 times lower than that from the as-grown heterostructure. Second, in our fabricated device, there is no high Q cavity formed (except the bottom DBR) for the entire PBG region. We also fabricated oxide-confined VCSEL-like devices (without any top mirror or PBG) and these devices

did not lase, confirming the fact that the observed output shown in Fig. 2 is from the defect microcavity. As a final proof of lasing from the microcavity, we performed near- and far-field measurements of the output. The results are shown in Fig. 3. A near-field image, of  $4\mu\text{m}$  lateral extent, which is much smaller than the oxide window diameter of  $40\mu\text{m}$ , is shown in Fig. 3a. The image indicates that the emission envelops the first few periods of the photonic crystal, with the double degenerate modal characteristics [8]. The measured far-field radiation patterns, with and without PBG formation, are shown in Fig. 3b. The linewidth narrows considerably in the latter case, confirming that lasing originates from the defect mode.

**Acknowledgment:** The work is supported by the Office of Naval Research.

© IEE 2000  
*Electronics Letters Online No: 20001131*  
 DOI: 10.1049/el:20001131

13 July 2000

W.D. Zhou, J. Sabarinathan, B. Kochman, E. Berg, O. Qasaimeh, S. Pang and P. Bhattacharya (Department of Electrical Engineering and Computer Science, University of Michigan, Ann Arbor, MI 48109-2122, USA)

## References

- 1 YOKOYAMA, H.: 'Physics and device applications of optical microcavities', *Science*, 1992, **256**, pp. 66–70
- 2 YABLONOVITCH, E.: 'Photonic band-gap structures', *J. Opt. Soc. Am. B*, 1993, **10**, pp. 283–295
- 3 VILLENEUVE, P., FAN, S., and JOANNOPOULOS, J.D.: 'Microcavities in photonic crystals: mode symmetry, tunability, and coupling efficiency', *Phys. Rev. B*, 1996, **54**, (11), pp. 7837–7842
- 4 BENISTY, H., WEISBUCH, C., LABILLOY, D., RATTIER, M., SMITH, C.J.M., KRAUSS, T.F., DE LA RUE, R.M., HOUDRE, R., OESTERLE, U., JOUANIN, C., and CASSAGNE, D.: 'Optical and confinement properties of two-dimensional photonic crystals', *J. Lightwave Technol.*, 1999, **17**, (11), pp. 2063–2077
- 5 LEE, R.K., PAINTER, O.J., KITZKE, B., SCHERER, A., and YARIV, A.: 'Photonic bandgap disk laser', *Electron. Lett.*, 1999, **35**, (7), pp. 569–570
- 6 HWANG, J., RYU, H., SONG, D., HAN, I.L., SONG, H., PARK, H., LEE, Y., and JANG, D.: 'Room-temperature triangular-lattice two-dimensional photonic bandgap lasers operating at  $1.54\mu\text{m}$ ', *Appl. Phys. Lett.*, 2000, **76**, (21), pp. 2982–2984
- 7 BERG, E., and PANG, S.W.: 'Cl<sub>2</sub> plasma passivation of etch induced damage in GaAs and InGaAs with an inductively coupled plasma source', *J. Vac. Sci. Tech. B*, 1999, **17**, pp. 2745–2749
- 8 PAINTER, O., VUCKOVIC, J., and SCHERER, A.: 'Defect modes of a two-dimensional photonic crystal in optically thin dielectric slab', *J. Opt. Soc. Am. B*, 1993, **10**, pp. 275–285